Implications of extinction due to meteoritic smoke in the upper stratosphere

Ryan R. Neely III,[1,2,3] Jason M. English,[1,4] Owen B. Toon,[1,4] Susan Solomon,[1] Michael Mills,[5] and Jeffery P. Thayer[6]

[1] Recent optical observations of aerosols in the upper stratosphere and mesosphere show significant amounts of extinction at altitudes above about 40 km where the stratospheric sulfate aerosol layer ends. Recent modeling of this region reveals that meteoritic smoke settling from the mesosphere and its interaction with the upper part of the sulfate aerosol layer is the origin of the observed extinction. Extinction in this region has major implications for the interpretation and analysis of several kinds of aerosol data (satellite and lidar). We compare observations from the SAGE II satellite and from NOAA's lidar located at Mauna Loa, Hawaii to extinction profiles derived from the Whole Atmosphere Community Climate Model (WACCM) coupled with the Community Aerosol and Radiation Model for Atmospheres (CARMA). Our results show that a major source of extinction exists in the region above about 30 km that must be addressed by all remote sensing instruments that have traditionally used the stratosphere above about 30 km as an aerosol free region to estimate the molecular component of their total extinction. It is also shown that meteoritic smoke not only contributes to but also becomes the dominant source of aerosol extinction above 35 km and poleward of 30 degrees in latitude, as well as above 40 km in the tropics. After addressing the concerns described here, current and past observations of this region could be reanalyzed to further our understanding of meteoritic dust in the upper stratosphere. **Citation:** Neely, R. R., III, J. M. English, O. B. Toon, S. Solomon, M. Mills, and J. P. Thayer (2011), Implications of extinction due to meteoritic smoke in the upper stratosphere, *Geophys. Res. Lett.*, *38*, L24808, doi:10.1029/2011GL049865.

1. Introduction

[2] *Hunten et al.* [1980], following on work by *Rosinski and Snow* [1961], suggested that evaporation and recondensation of much of the approximately 40 tons of micrometeors ablating in the atmosphere each day would lead to nanometer-sized smoke particles near the mesopause. They suggested that these particles would slowly coagulate to larger sizes and drift downward, creating a relatively uniform smoke layer that extends into the lower stratosphere. While numerical models of the properties of the particles have been constructed [e.g., *Megner et al.*, 2008; *Bardeen et al.*, 2008], and numerous rocket soundings have probed them, it is only recently that optical observations of meteoritic smoke in the mesosphere and upper stratosphere (35 to 85 km) have confirmed their existence [*Hervig et al.*, 2009]. Here we show that these particles provide a major source of optical extinction in the upper stratosphere that remote sensing instruments currently ignore when attempting to separate the amount of extinction due aerosols from the molecular component of their total observed extinction. Omitting this component of the total extinction leads to biases in retrieved extinction profiles throughout the stratosphere because it leads to an over-estimate of the molecular extinction. Consequently, a recalibration is necessary for measurements that determine aerosol extinction based on fitting observations to density profiles at altitudes where the atmosphere is incorrectly assumed to be "clean" (purely molecular). *Vernier et al.* [2009] demonstrate such a recalibration for the CALIPSO dataset. However, *Vernier et al.* [2009] did not identify the species of aerosol responsible for the observed extinction within the original calibration range, which is the focus of the present study. It is also noted that when these concerns have been addressed, current datasets hold the potential to reveal new information about meteoritic smoke.

[3] *Rosen* [1964] first postulated that meteoritic material might compose some of the stratospheric aerosols below 30 km, based on observations using photoelectric counters on balloons. These first-reported observations of meteoritic stratospheric aerosol suggested large fluxes of meteoritic material into the atmosphere. During this same time, the first lidar measurements were motivated by observations that suggested layers of aerosol existed above 60 km [*Fiocco and Smullin*, 1963; *Clemesha et al.*, 1967]. These layers were attributed to the break up of meteoroids and the descent of the subsequent particles [*Fiocco and Colombo*, 1964]. Though it was later found that these observations may have been erroneous due to the interference from the instrument [*Bain and Sandford*, 1966], it is interesting to note the importance of meteoritic smoke in lidar observations since their beginnings.

[4] *Hunten et al.* [1980] produced an initial model of the distribution of the micrometeorites from the mesosphere to the stratosphere, while *Turco et al.* [1981] showed from models that meteoritic debris could represent an important natural aerosol constituent of the stratosphere and would affect the observable properties of stratospheric aerosols.

[1]Department of Atmospheric and Oceanic Sciences, University of Colorado, Boulder, Colorado, USA.
[2]Earth Systems Research Laboratory, National Oceanic and Atmospheric Administration, Boulder, Colorado, USA.
[3]Cooperative Institute for Research in Environmental Sciences, Boulder, Colorado, USA.
[4]Laboratory for Atmospheric and Space Physics, University of Colorado, Boulder, Colorado, USA.
[5]Earth System Laboratory, National Center for Atmospheric Research, Boulder, Colorado, USA.
[6]Department of Aerospace Engineering Sciences, University of Colorado, Boulder, Colorado, USA.
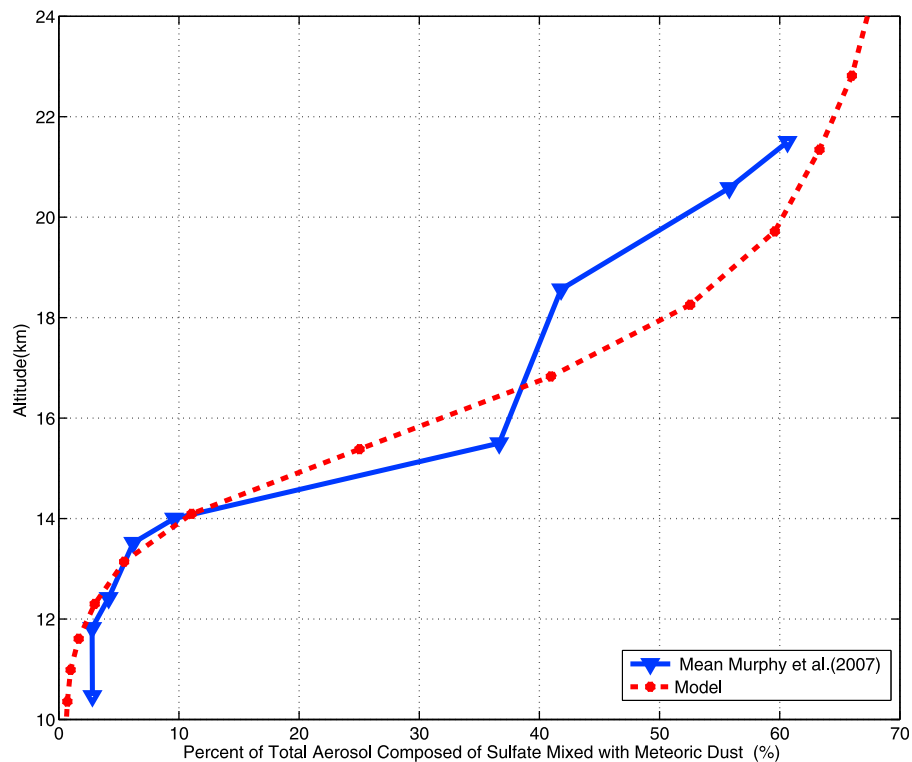
Figure 1. Comparison of the fraction of mixed sulfate-meteoritic smoke aerosol to total aerosol by number between the model and observations reported by *Murphy et al.* [2007].

The first global and temporal study of meteoritic smoke was conducted by *Megner et al.* [2008] using a two-dimensional model. This study showed the inadequacies of the simplification used by previous one-dimensional models due to the latitudinal and season dependence of the distribution of the meteoritic smoke. *Bardeen et al.* [2008] conducted the first three-dimensional modeling of meteoritic smoke and showed that the mesospheric meridional circulation may create strong and seasonally varying latitudinal gradients in the meteoritic smoke because of rapid transport downward into the stratosphere in the winter polar vortices, where smoke particles may participate in the nucleation of sulfate aerosols and influence the formation of polar stratospheric clouds.

[5] Recent *in situ* observations in the lower stratosphere made by *Murphy et al.* [1998, 2007] demonstrate that the meteoritic component of stratospheric aerosol is significant during volcanically quiescent periods. More than 50% of aerosol contains magnesium and iron at about 20 km and this fraction becomes more significant higher in the stratosphere (Figure 1) [*Murphy et al.*, 2007]. This altitude trend is consistent with a meteoritic source. This has been confirmed by the recent work of *Hervig et al.* [2009] who show the first observations of meteoritic smoke in the upper atmosphere derived from remote sensing instruments.

[6] Here we show the need for the inclusion of these particles when retrieving observations of the sulfate aerosol layer in the lower stratosphere (15 km to 40 km) with remote sensing instruments. Model-derived aerosol extinction profiles, with and without meteoritic smoke, are compared to profiles observed by SAGE II [*Chu et al.*, 1989] and by the NOAA Global Monitoring Division's lidar located in Mauna Loa, HI [*Barnes and Hofmann*, 1997, 2001; *Hofmann et al.*, 2003, 2009]. These comparisons show that meteoritic smoke contributes a significant proportion to the observed aerosol extinction in the upper stratosphere. Descending through the atmosphere, extinction by smoke is initially dominated by absorption, but scattering by mixed smoke-sulfate aerosols becomes the dominant process below about 32 km. In this second case the smoke particles cause the sulfate layer to have a larger number of relatively smaller sulfate aerosol particles. This allows the particles to have longer residence times and increase the total abundance of aerosol at these altitudes [*Turco et al.*, 1981]. It is also noted that the entire SAGE II extinction record (1984–2005) displays noticeable extinction in the region above 30 km, though the cause of the extinction has not previously been recognized as meteoritic smoke particles.

2. Model Description

[7] We use the Whole Atmosphere Community Climate Model (WACCM) [*Garcia et al.*, 2007] coupled with the Community Aerosol and Radiation Model for Atmospheres (CARMA) [*Toon et al.*, 1988]. The application of the coupled WACCM/CARMA model to stratospheric aerosols is described by *English et al.* [2011]. Although CARMA is capable of interacting radiatively and chemically with WACCM, for these studies the interactions were mainly disabled. This version of WACCM utilizes SAGE II sulfate surface area densities for radiative transfer and ozone heterogeneous chemistry calculations. Further description of the specific setup of WACCM and CARMA used in this study may be found in the auxiliary material.[1]
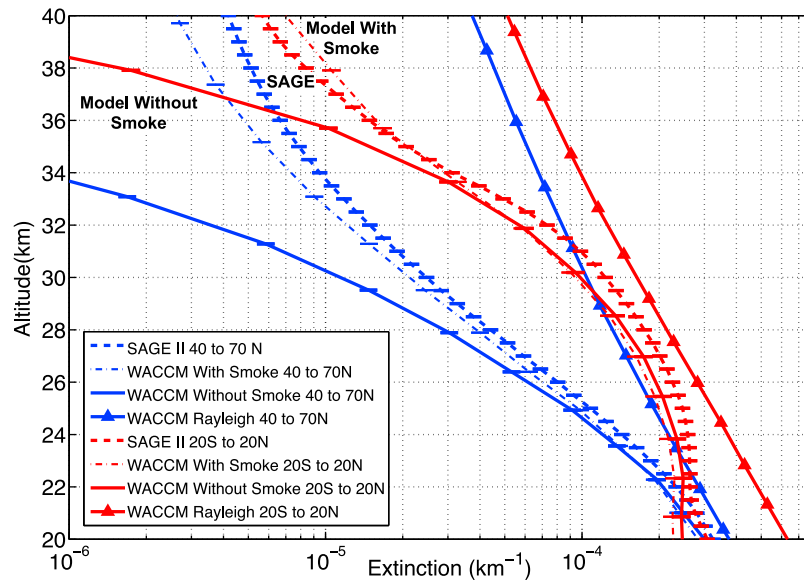
Figure 2. Globally averaged model aerosol extinction profiles (525 nm) are compared to aerosol extinction profiles (total extinction profiles with Rayleigh scattering subtracted) from Stratospheric Aerosol and Gas Experiment (SAGE) II satellite retrievals [*Chu et al.*, 1989] at a wavelength of 525 nm. The SAGE data are averaged from years 2000–2005. Simulations are 10-yr averages. WACCM data points have been converted from a vertical model pressure grid to geometric altitudes (using model derived temperature profiles) for the comparison. The Rayleigh scattering lines are shown as a comparison for the amount of scattering caused by the molecular atmosphere.

[8] The meteoritic smoke in this model is based on the work of *Bardeen et al.* [2008]. Previous studies of micro-meteorite ablation are used to specify the altitude of the emission and the amount of mass emitted as described by *Bardeen et al.* [2008]. The formation of smoke is represented in the model as a constant source of particles emitted globally into the smallest smoke aerosol size bin between the altitude levels of 0.01 hPa (75 km) and 0.0001 hPa (110 km) (see the auxiliary material for details). For this work, the composition of meteoritic smoke is important because the refractive index depends strongly on the particle composition. Observations and modeling suggest that meteoritic smoke is optically similar to a mixture of olivine and hematite [*Hervig et al.*, 2009]. Based on *Hervig et al.* [2009], this work assumes a 75%/25% mixture of olivine and hematite, and uses a linear combination of the appropriate optical constants from the work of *Jäger et al.* [2003] and *Huffman and Stapp* [1973]. The index of refraction for the sulfate aerosols is better understood due to the less complex composition of the aerosol (binary sulfuric acid and water). As suggested by *Palmer and Williams* [1975], the real part of the index of refraction at visible wavelengths is allowed to vary as a function of the weight percent of sulfuric acid. Absorption by the sulfate aerosol is insignificant due to the small imaginary component of the refractive index of sulfuric acid at visible wavelengths and is not considered in the calculations shown here. The mixed sulfate population is modeled as homogenous particles using the same index of refraction as the pure sulfate population. This was done rather than modeling the particles as concentric spheres because the impact of the smoke particle core, which increases the absorption of the aerosol, is negligible compared to the scattering caused by the larger sulfate mantle [*Bohren and Huffman*, 1983]. All Mie calculations used to determine aerosol extinction and backscatter in this analysis use *Bohren and Huffman*'s [1983]

algorithms that were adapted for use in MATLAB by *Mätzler* [2002] and assume that the particles are spheres.

3. Observation-Model Comparison

[9] In Figure 1, we compare the vertical profile of the fraction of the aerosols containing smoke from annually averaged model simulations to the observations presented by *Murphy et al.* [2007]. The *in situ* measurements reported by *Murphy et al.* [1998, 2007] suggest that the meteoritic component of stratospheric aerosol increases with height. The observations come from three aircraft measurement campaigns flown from Houston, TX, Key West, FL and San Jose, Costa Rica onboard the NASA WB-57F, which we averaged. Model output is averaged over a similar geographic region as the observations. Measurements represent the fraction of the total number of particles that have positive ions from both sulfate and meteoritic smoke (as defined by *Murphy et al.* [2007]). The model fraction is derived from the total number of particles contained in the mixed sulfate-smoke size bins compared to the total number of aerosols (only particles with wet radii larger than 300 nm were counted from the model in order to match the detection ability of the instruments used by *Murphy et al.* [2007]), including those that are pure sulfates. The comparison displays overall agreement and demonstrates the model's ability to capture the increasing importance of meteoritic smoke with height and the complexities of the interactions of meteoritic smoke with sulfate aerosol.

[10] In Figure 2, model calculations that include and exclude meteoritic smoke are compared to SAGE II aerosol extinction retrievals averaged from 2000 to 2005 in the tropics (20°S to 20°N) and northern mid-latitudes (45°N to 70°N). Both sets of model output compare well to SAGE II observations between 20 and 30 km. This suggests that
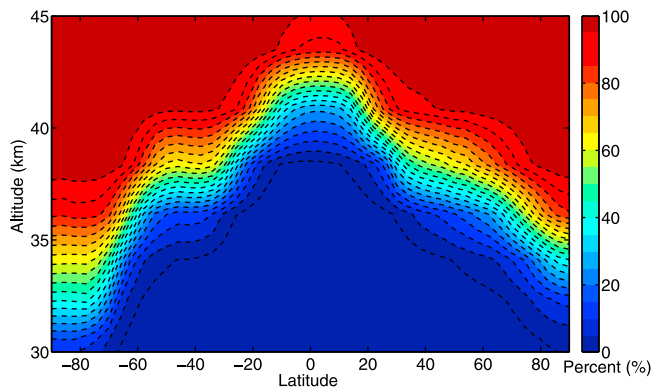
Figure 3. Percentage of modeled zonal average total aerosol extinction at 532 nm due to meteoritic smoke alone. This was calculated by taking the ratio of the extinction caused by meteoritic smoke particles alone to the total amount of extinction from all aerosols (meteoritic smoke plus mixed and pure sulfates) included in the model. Average comes from 10 years of model run time.

sulfates dominate aerosol extinction in this region. However, above 30–35 km the two models diverge beyond the standard deviation of the observations in the mid-latitudes. The model including the smoke source much more closely resembles the observations above 30–35 km. The model without smoke diverges from the SAGE II observations at a lower altitude in mid-latitudes than in the tropics. The southern hemisphere follows similar trends to the northern hemisphere, but is on average 15% lower in the amount of extinction caused by aerosol.

[11] This latitude dependence is further illustrated in Figure 3, which depicts the zonal averaged percentage of extinction due to meteoritic smoke compared to the total amount of extinction due to all aerosols in the model (meteoritic, mixed sulfate-meteoritic, and pure sulfates). Poleward of 30° in latitude, the role of meteoritic smoke above 35 km is significant. In the tropics, meteoritic smoke dominates above about 40 km. Of course the smoke also modifies the extinction due to the mixed particles, which is not included in Figure 3. As can be judged from Figure 2, adding smoke changes the extinction at mid-latitudes by about a factor of 2 at 25 km. Much of this change comes from the impact of meteoritic smoke particles on the observable properties of the sulfate aerosol.

[12] In Figure 4, modeled aerosol backscatter coefficients and derived lidar aerosol backscatter coefficients are compared to demonstrate how neglecting the impact of meteoritic smoke can lead to an underestimate of the scattering due to aerosols. The aerosol backscatter is determined by subtracting the Rayleigh backscatter from the total observed backscatter. We have included a model derived Rayleigh backscatter profile to demonstrate the total amount of backscatter expected in an aerosol-free atmosphere. The lidar profiles are mean profiles taken from data spanning from 2000 to 2010 with major volcanic influences filtered out. Modeled profiles come from an average of ten years of model simulation.

[13] In this comparison, the original lidar profile most closely resembles the modeled profile without smoke emissions. The model aerosol backscatter including smoke exceeds the original lidar-retrieved aerosol backscatter

above 25 km, suggesting the current retrieval underestimates the amount of aerosol scattering. This result is a consequence of the lidar aerosol retrieval method. The procedure used by the Mauna Loa aerosol lidar to separate the aerosol component of the backscatter from the molecular part was pioneered by *Fernald et al.* [1972] and *Klett* [1981] and is in wide use within the lidar community [*Russell et al.*, 1979; *Thayer et al.*, 1997; *Hofmann et al.*, 2003; *Pappalardo et al.*, 2004]. The method uses an altitude range near the top of the raw lidar backscatter profile (determined by a trade off between signal strength and where aerosol impacts were thought to be negligible) to provide a reference point for a molecular density profile derived from a model or other observations. The adjusted Rayleigh profile is then projected down through the lower altitudes of the backscatter profile and any deviations of the actual lidar profile from the calibrated Rayleigh profile may be attributed to aerosols. *Russell et al.* [1979] showed how small deviations in the top of the profile used to derive the molecular profile, attributed to aerosol scattering, can cause definite biases in the aerosol profiles. *Russell et al.* [1979] also show that including a small correction to account for additional aerosol scattering at the calibration altitude can improve the retrieved aerosol profiles, as compared to those obtained when the topside calibration altitude is erroneously assumed to be aerosol free. Furthermore, recent observations from the CALIPSO lidar by *Vernier et al.* [2009] suggest an increase in aerosol to Rayleigh ratio in the tropical stratosphere that ranges from 2-12% with an average of 6%. Based on these observations and model results, we apply an 8% adjustment to the calibration region between 35 to 40 km.

[14] In Figure 4, the impact of the adjustment in the retrieval process as suggested by *Russell et al.* [1979] and *Vernier et al.* [2009] is evident. The modeled aerosol
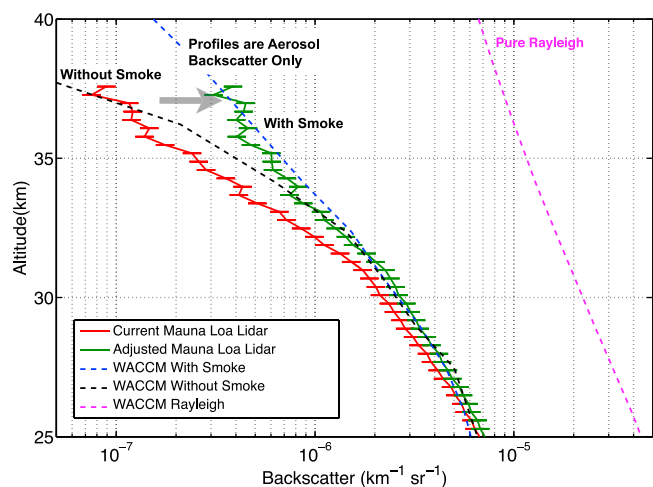

Figure 4. Comparison of the NOAA Mauna Loa, HI lidar aerosol backscatter (total backscatter minus Rayleigh backscatter) averaged from 2000 to 2010 to mean aerosol backscatter profiles derived from 10 years of model simulations, with and without the meteoritic smoke source, taken from the model grid box closest to Mauna Loa. Error bars represent 1σ standard deviation. The arrow represents the altitude where an 8% adjustment to the calibration scattering ratio was made to the original lidar data to account for the presence of meteoritic smoke.

backscatter when smoke is included now more closely compares to the lidar observations, suggesting that such an adjustment is required to take into account the effect of meteoritic smoke at the lidar calibration altitude. While the altitude level at which meteoritic smoke dominates the extinction declines with increasing latitude as shown in Figure 2, the altitude at which lidars chose to determine their molecular profile is also lower at higher latitudes. Hence we conclude that most stratospheric lidars are generally not correctly attributing the extinction observed above 30 km to the correct source.

[15] While we have concentrated in this paper on discussing the role of meteoritic smoke above 30 km on lidar observations, *English et al.* [2011] show that the models also tend to depart from the data below 20 km. There are several reasons for these departures as discussed by *English et al.* [2011]. The observations presented by *Murphy et al.* [2007] suggest that differences between models and observations from SAGE II and lidar in the section of the profile from the tropopause to 20km could be due to the exclusion of carbonaceous aerosols in model. Carbonaceous aerosols have tropospheric sources and may account for a significant fraction of the total aerosol in this region.

4. Summary and Discussion

[16] Comparisons of observations to model derived extinction profiles in the stratosphere with and without the inclusion of smoke suggest that the extinction caused by meteoritic smoke and its interaction with the sulfate aerosol is significant down to altitudes as low as 25-30 km at midlatitudes and 35 km in the tropics. Hence the presence of the smoke needs to be considered in remote sensing retrievals. When this extinction is omitted, lidar measurements appear to be biased through a significant depth of the stratosphere, down to near 30 km in the tropics.

[17] The radiative forcing of the meteoritic smoke has not been fully explored but is thought to be insignificant compared to the amount of forcing caused by lower stratosphere aerosols reported for example by *Solomon et al.* [2011]. Based on the recalibration of CALIPSO by *Vernier et al.* [2009], we assume the error in backscatter from improperly calibrating lidar data is on the order of 8-12%. This value also corresponds to the amount of adjustment in the recalibration of the lidar profile in Figure 4 needed to match the modeled aerosol. This change in scattering suggests that if the results of *Solomon et al.* [2011] had used the unadjusted CALIPSO data the amount of cooling attributed to extinction from the stratosphere since 2000 would have been reduced by $\sim$5% ($\sim$0.01 W/m^2). Possible solutions to achieve more accurate calibration include calibrating instruments within regions of the atmosphere in which information about the extinction of meteoritic aerosol is known and may be included within retrievals. SAGE and other similar observations (including lidar observations after addressing the concerns described in this work) above about 30 km altitude reflect the behavior of meteoritic smoke, and could be mined to learn more about temporal trends and latitudinal behavior of meteoritic smoke as well as its impact upon the sulfate aerosol layer.

References

Bain, W., and M. C. W. Sandford (1966), Light scatter from a laser beam at heights above 40 km, *J. Atmos. Terr. Phys.*, 28, 543–552, doi:10.1016/0021-9169(66)90068-7.

Bardeen, C. G., O. B. Toon, E. J. Jensen, D. R. Marsh, and V. L. Harvey (2008), Numerical simulations of the three-dimensional distribution of meteoritic dust in the mesosphere and upper stratosphere, *J. Geophys. Res.*, 113, D17202, doi:10.1029/2007JD009515.

Barnes, J. E., and D. J. Hofmann (1997), Lidar measurements of stratospheric aerosol over Mauna Loa Observatory, *Geophys. Res. Lett.*, 24(15), 1923–1926, doi:10.1029/97GL01943.

Barnes, J. E., and D. J. Hofmann (2001), Variability in the stratospheric background aerosol over Mauna Loa Observatory, *Geophys. Res. Lett.*, 28(15), 2895–2898, doi:10.1029/2001GL013127.

Bohren, C. F., and D. R. Huffman (1983), *Absorption and Scattering of Light by Small Particles*, Wiley-Intersci., New York.

Chu, W. P., M. P. McCormick, J. Lenoble, C. Brogniez, and P. Pruvost (1989), SAGE II inversion algorithm, *J. Geophys. Res.*, 94(D6), 8339–8351, doi:10.1029/JD094iD06p08339.

Clemesha, B. R., G. S. Kent, and R. W. H. Wright (1967), Optical radar evidence for atmospheric dust layers around 85 km altitude, *Nature*, 214, 261–262, doi:10.1038/214261b0.

English, J. M., O. B. Toon, M. J. Mills, and F. Yu (2011), Microphysical simulations of new particle formation in the upper troposphere and lower stratosphere, *Atmos. Chem. Phys.*, 11, 9303–9322, doi:10.5194/acp-11-9303-2011.

Fernald, F. G., B. M. Herman, and J. A. Reagan (1972), Determination of aerosol height distributions by lidar, *J. Appl. Meteorol.*, 11, 482–489, doi:10.1175/1520-0450(1972)011<0482:DOAHDB>2.0.CO;2.

Fiocco, G., and G. Colombo (1964), Optical radar results and meteoric fragmentation, *J. Geophys. Res.*, 69(9), 1795–1803, doi:10.1029/JZ069i009p01795.

Fiocco, G., and L. D. Smullin (1963), Detection of scattering layers in the upper atmosphere (60–140 km) by optical radar, *Nature*, 199, 1275–1276, doi:10.1038/1991275a0.

Garcia, R. R., D. R. Marsh, D. E. Kinnison, B. A. Boville, and F. Sassi (2007), Simulation of secular trends in the middle atmosphere, 1950–2003, *J. Geophys. Res.*, 112, D09301, doi:10.1029/2006JD007485.

Hervig, M. E., L. L. Gordley, L. E. Deaver, D. E. Siskind, M. H. Stevens, J. M. Russell III, S. M. Bailey, L. Megner, and C. G. Bardeen (2009), First satellite observations of meteoric smoke in the middle atmosphere, *Geophys. Res. Lett.*, 36, L18805, doi:10.1029/2009GL039737.

Hofmann, D. J., J. E. Barnes, E. Dutton, T. Deshler, H. Jäger, R. Keen, and M. Osborn (2003), Surface-based observations of volcanic emissions to the stratosphere, in *Volcanism and the Earth's Atmosphere, Geophys. Monogr. Ser.*, vol. 139, edited by A. Robock and C. Oppenheimer, pp. 57–73, AGU, Washington, D. C., doi:10.1029/139GM04.

Hofmann, D. J., J. E. Barnes, M. O'Neill, M. Trudeau, and R. R. Neely (2009), Increase in background stratospheric aerosol observed with lidar at Mauna Loa Observatory and Boulder, Colorado, *Geophys. Res. Lett.*, 36, L15808, doi:10.1029/2009GL039008.

Huffman, D. R., and J. L. Stapp (1973), Optical measurements on solids of possible interstellar importance, in *Interstellar Dust and Related Topics*, edited by J. Mayo Greenberg and H. C. van de Hulst, pp. 297–301, Reidel, Dordrecht, Netherlands.

Hunten, D. M., R. P. Turco, and O. B. Toon (1980), Smoke and dust particles of meteoric origin in the mesosphere and stratosphere, *J. Atmos. Sci.*, 37, 1342–1357, doi:10.1175/1520-0469(1980)037<1342:SADPOM>2.0.CO;2.

Jäger, C., V. B. Il'in, T. Henning, H. Mutschke, D. Fabian, D. A. Semenov, and N. V. Voshchinnikov (2003), A database of optical constants of cosmic dust analogs, *J. Quant. Spectrosc. Radiat. Transfer*, 79-80, 765–774, doi:10.1016/S0022-4073(02)00301-1.

Klett, J. (1981), Stable analytical inversion solution for processing lidar returns, *Appl. Opt.*, 20(2), 211–220, doi:10.1364/AO.20.000211.

Mätzler, C. (2002), MATLAB functions for Mie scattering and absorption, *Res. Rep. 2002-08*, Inst. für Angew. Phys., Hamburg, Germany.

Megner, L., D. E. Siskind, M. Rapp, and J. Gumbel (2008), Global and temporal distribution of meteoric smoke: A two-dimensional simulation study, *J. Geophys. Res.*, *113*, D03202, doi:10.1029/2007JD009054.

Murphy, D. M., D. S. Thomson, and M. J. Mahoney (1998), In situ measurements of organics, meteoritic material, mercury, and other elements in aerosols at 5 to 19 kilometers, *Science*, *282*(5394), 1664–1669, doi:10.1126/science.282.5394.1664.

Murphy, D. M., D. J. Cziczo, P. K. Hudson, and D. S. Thomson (2007), Carbonaceous material in aerosol particles in the lower stratosphere and tropopause region, *J. Geophys. Res.*, *112*, D04203, doi:10.1029/2006JD007297.

Palmer, K. F., and D. Williams (1975), Optical constants of sulfuric acid; application to the clouds of Venus?, *Appl. Opt.*, *14*, 208–219.

Pappalardo, G., et al. (2004), Aerosol lidar intercomparison in the framework of the EARLINET project. 3. Raman lidar algorithm for aerosol extinction, backscatter, and lidar ratio, *Appl. Opt.*, *43*(28), 5370–5385, doi:10.1364/AO.43.005370.

Rosen, J. M. (1964), The vertical distribution of dust to 30 kilometers, *J. Geophys. Res.*, *69*(21), 4673–4676, doi:10.1029/JZ069i021p04673.

Rosinski, J., and R. H. Snow (1961), Secondary particulate matter from meteor vapors, *J. Atmos. Sci.*, *18*, 736–745.

Russell, P. B., T. J. Swissler, and M. P. McCormick (1979), Methodology for error analysis and simulation of lidar aerosol measurements, *Appl. Opt.*, *18*(22), 1–15, doi:10.1364/AO.18.003783.

Solomon, S., J. S. Daniel, R. R. Neely, J. P. Vernier, E. G. Dutton, and L. W. Thomason (2011), The persistently variable "background" stratospheric aerosol layer and global climate change, *Science*, *333* (6044), 866–870, doi:10.1126/science.1206027.

Thayer, J., N. Nielsen, R. Warren, C. Heinselman, and J. Sohn (1997), Rayleigh lidar system for middle atmosphere research in the Arctic, *Opt. Eng.*, *36*(7), 2045–2061, doi:10.1117/1.601361.

Toon, O. B., R. P. Turco, D. L. Westphal, R. Malone, and M. S. Liu (1988), A multidimensional model for aerosols: Description of computational analogs, *J. Atmos. Sci.*, *45*(15), 2123–2144, doi:10.1175/1520-0469(1988) 045<2123:AMMFAD>2.0.CO;2.

Turco, R. P., O. B. Toon, P. Hamill, and R. C. Whitten (1981), Effects of meteoritic debris on stratospheric aerosols and gases, *J. Geophys. Res.*, *86*(C2), 1113–1128, doi:10.1029/JC086iC02p01113.

Vernier, J. P., et al. (2009), Tropical stratospheric aerosol layer from CALIPSO lidar observations, *J. Geophys. Res.*, *114*, D00H10, doi:10.1029/2009JD011946.

J. M. English, R. R. Neely III, S. Solomon, and O. B. Toon, Department of Atmospheric and Oceanic Sciences, University of Colorado, Boulder, CO 80309-0392, USA. (ryan.r.neely@noaa.gov)

M. Mills, Earth System Laboratory, National Center for Atmospheric Research, PO Box 3000, 487 Boulder, CO 80307-3000, USA.

J. P. Thayer, Department of Aerospace Engineering Sciences, University of Colorado, Boulder, CO 80309-0429, USA.